

A Low-Cost, Rapid Deposition Method for “Smart” Films: Applications in Mammalian Cell Release

Jamie A. Reed, Adrienne E. Lucero, Steve Hu, Linnea K. Ista, Mangesh T. Bore, Gabriel P. López, and Heather E. Canavan*

Center for Biomedical Engineering, Department of Chemical and Nuclear Engineering, University of New Mexico, Albuquerque, New Mexico 87131-1141

ABSTRACT The “smart” polymer poly (*N*-isopropyl acrylamide), or pNIPAM, has been studied for bioengineering applications. The polymer’s abrupt change in hydrophobicity near physiologic temperatures makes it ideal for use as a substrate in many applications, including protein separation and prevention of biofouling. To tether pNIPAM, many techniques such as plasma deposition, have been utilized, but most are expensive and require long equipment calibration or fabrication periods. Recently, a novel method for codepositing this smart polymer with a sol–gel, tetraethyl orthosilicate (TEOS), was developed. In this work, we adapt this technique for applications in mammalian cell attachment/detachment. In addition, we compare the effects of the pNIPAM/TEOS ratio to functionality using surface analysis techniques (XPS and contact angles). We found the optimal ratio to be 0.35 wt % pNIPAM/TEOS. Cell detachment from these substrates indicate that they would be ideal for applications that do not require intact cell sheets, such as biofouling prevention and protein separation, as this technique is a simple and affordable technique for pNIPAM deposition.

KEYWORDS: cell • detachment • sol–gel • NIPAM • thermoresponsive • XPS

INTRODUCTION

Poly(*N*-isopropyl acrylamide), or pNIPAM, is a “smart” polymer that has been studied extensively for the reversible adhesion of mammalian cells (1–3). It has been demonstrated that many mammalian cell types attach to grafted pNIPAM in a similar fashion as when exposed to tissue culture polystyrene (TCPS): the cells proliferate into a confluent sheet (4, 5). However, when the temperature of the cell culture is lowered below the lower critical solution temperature (LCST) of the polymer (~32 °C), the cells detach and can be harvested for tissue engineering applications. This is in contrast to cells grown on TCPS, which will not detach because of a decrease in temperature, requiring enzymatic digestion (via trypsin) or mechanical scraping to remove them (1, 5, 6).

In addition to tissue engineering applications, this “smart” polymer has also been utilized for the controlled attachment and release of bacteria (7, 8), biosensors (9), and tissue engineering (10). All of these applications first require the deposition of pNIPAM onto a cell culture substratum.

There are many methods used to polymerize NIPAM, such as free radical polymerization using a variety of initiators and solvents (11–13) or redox initiation using a variety of initiators and accelerators (14, 15). Free radical polymerization, or ATRP, has the advantages of mild reaction conditions, the ability to use a wide range of monomers, and

insensitivity to impurities, such as water, that are present during the reaction (16, 17). Electron beam irradiation is a process that can be completed in mild conditions (e.g., room temperature, in water, at physiological pH), allows for high depth penetration, and does not need cross-linking or initiator agents (18). The disadvantages to the techniques described above are that the surface that is coated usually has to be a flat surface (in the case of pouring and drying a solution (19)), or is dependent upon a specific surface chemistry (in the case of activated substrates (20) and ATRP (21)). A review of some common deposition methods used for to create pNIPAM films was recently published by Da Silva (22).

Most of the aforementioned methods require expensive equipment and long deposition times. In addition, system calibration for these methods can be extensive and time intensive. Recently, Rao et al patented a novel low-cost method for the rapid codeposition of pNIPAM with a tetraethyl orthosilicate (TEOS) based sol–gel (23, 24). In this work, we adapt this technique for the reversible adhesion of mammalian cells, and explore its applications for bioengineering. Following characterization of these substrates using traditional surface chemistry techniques (e.g., X-ray photoelectron spectroscopy, XPS; and contact angle measurements), identical populations of bovine aortic endothelial cells (BAECs) were grown to confluence on treated glass slides. From these results, we concluded that 0.35 wt % pNIPAM/TEOS (or 0.35 wt % spNIPAM) surfaces demonstrated the best thermoresponse and cellular response, thus generating affordable pNIPAM substrates up to 4 times faster than the previously mentioned methods. In addition, the

* Corresponding author. Tel: (505) 277-8026. Fax: (505) 277-5433. E-mail: canavan@unm.edu.

Received for review November 24, 2009 and accepted February 22, 2010

DOI: 10.1021/am900821t

© 2010 American Chemical Society

current method requires only TEOS, pNIPAM, and minor instrumentation (spin coater, ~\$5000) compared to ~\$35 000 for an RF plasma reactor.

EXPERIMENTAL METHODS

The pNIPAM (molecular weight of ~40 000) was purchased from Polysciences, Inc. (Warrington, PA). The tetraethyl orthosilicate (TEOS) was purchased from Sigma-Aldrich (St. Louis, MO). The round glass coverslips were 15 mm in diameter and were purchased from Ted Pella, Inc. (Redding, CA). The silicon chips were obtained from Silitec (Salem, OR). The 200 proof ethanol, HPLC grade methanol, HPLC grade dichloromethane, and hydrochloric acid were purchased from Honeywell Burdick & Jackson (Deer Park, TX). The acetone was purchased from Fisher Scientific (Pittsburgh, PA).

The cell culture media was from Cellgro (Manassas, VA). Bovine aortic endothelial cells (BAECs) were from Genlantis (San Diego, CA) and cultured in 24-well tissue culture polystyrene (TCPS) plates from Greiner Bio-one (Monroe, NC). The DPBS without calcium-chloride or magnesium-chloride was purchased from HyClone (Logan, UT). The 0.25% trypsin-EDTA was from Gibco (Carlsbad, CA).

Statistically relevant data were obtained by replicating all procedures three times. Each replication of the experiment utilized three surfaces, with each surface analyzed in three different sites along the surface. This method was used for both surface analysis and cell behavior studies. A student t-test was used to verify statistical relevance.

Surface Preparation. Glass coverslips used for cell culture were cleaned with an acid wash (1:1 vol HCl:MeOH), rinsed with deionized water, and dried with nitrogen. Silicon chips used for surface analysis were washed with 10 min intervals in dichloromethane, acetone, and then methanol in an ultrasonic cleaner from VWR International (Brisbane, CA).

Sol–Gel and pNIPAM Preparation. Thirty-five mg of pNIPAM, 5 mL of distilled water, and 200 μ L of 1 Normal HCl were mixed, and a weight percentage of pNIPAM was determined. This solution is referred to as “pNIPAM only.” In a separate container, 250 μ L TEOS sol (1 TEOS:3.8 ethanol:1.1 water:0.0005 HCl), 43 μ L of distilled water, and 600 μ L of ethanol were mixed and weighed. This solution is referred to as “TEOS only.” To obtain different weight percentages of pNIPAM in sol, we added the appropriate amount of the pNIPAM solution to the pure TEOS in order to achieve the desired weight percentages for spNIPAM surfaces (e.g., 3.5 g of pNIPAM solution added to 996.5 g of TEOS sol).

Sol and pNIPAM Deposition. One-hundred to two-hundred microliters of the prepared solution was evenly distributed on clean surfaces placed on a spin coater, model 100 spinner from Brewer Science, Inc. (Rolla, MO). These surfaces were then spun at 2000 rpm for 60s. The surfaces were stored under nitrogen in a Parafilm-covered Petri dish until used for either (a) surface analysis or (b) cell culture tests.

Contact Angle. An Advanced Goniometer model 300-UPG (ramé-hart instrument co., Mountain Lakes, NJ) with an environmental chamber and DROPimage Standard program was used to measure inverted bubble contact angles in Ultrapure water (18 M Ohm cm). Contact angles were taken at room temperature and 37 °C using the Temp Controller model 100–500 connected to the environmental chamber. For contact angle data, the temperature below the LCST used was 25 °C instead of 4 °C (as was used in cell culture). This is because maintaining the goniometer at temperatures below the room temperature for an entire set of experiments (~30 min) is not feasible. In addition, we previously showed that for contact angle analysis below the LCST, the exact temperature does not affect the results (2).

X-ray Photoelectron Spectroscopy (XPS). All XPS spectra were taken on a Kratos Axis-Ultra DLD spectrometer. This

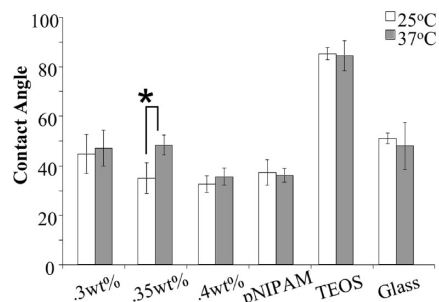


FIGURE 1. Contact angles show hydrophobicity change due to temperature shift from room temperature (25 °C in white) to culture temperature (37 °C in gray). A statistically significant change is demonstrated on 0.35 wt % spNIPAM surfaces, indicated with an asterisk.

instrument has a monochromatized Al K α X-ray and a low-energy electron flood gun for charge neutralization. X-ray spot size for these acquisitions was on the order of 300 \times 700 μ m (Kratos “Hybrid” mode). Pressure in the analytical chamber during spectral acquisition was $\sim 5 \times 10^{-9}$ Torr. The pass energy for survey spectra was 80 eV and the pass energy was 20 eV for high-resolution spectra (carbon).

Data treatment was performed on CasaXPS software (Manchester, UK). Core-level spectra were peak fit using the minimum number of peaks possible to obtain random residuals. A 70% Gaussian/30% Lorentzian line shape was used to fit the peaks, and a linear function was used to model the background.

Cell Culture. BAECs were cultured in Dulbecco’s Modified Eagle Medium supplemented with 10% fetal bovine serum, 1% penicillin/streptomycin, 4.5 g/L glucose, 0.1 mM MEM nonessential amino acids, and 1 mM MEM sodium pyruvate. Cells were incubated at 37 °C in a humid atmosphere with 5% CO₂. Cells were washed with Dulbecco’s phosphate buffered saline and lifted from culture flasks with 0.25% trypsin to seed 24-well plates with inserted pNIPAM deposited and blank control cover glass.

Cell Detachment. BAECs were cultured until confluence (approximately 4 days for these substrates). The medium was removed, and 4 °C serum-free media was added to each well. A previous investigation indicated using 4 °C serum-free media facilitated the fastest release of BAECs from pNIPAM (2). The culture plate was then placed on a shaker platform for 2 h and observed via light microscopy (Nikon F100, Melville, NY) with a 20 \times objective to determine the percentage of cells detached. Images were captured using Spot Advanced software (Sterling Heights, MI).

RESULTS AND DISCUSSION

Characterization of Surfaces. The spNIPAM surfaces are composed of a sol–gel (TEOS) and pNIPAM. To effect mammalian cell release, we needed to verify that the LCST occurred between room temperature (~25 °C) and cell culture temperature (~37 °C). Contact angle measurements, shown in Figure 1, indicate that there is a difference in the wettability of spNIPAM surfaces when the temperature is shifted from above the LCST (i.e., 37 °C) to below the LCST (i.e., 25 °C). However, the only statistically significant change, $13^\circ \pm 7$, was seen on 0.35 wt % spNIPAM surfaces. As expected, TEOS and control surfaces showed no statistically significant changes. The absence of a statistically significant contact angle change on the other surfaces suggests a lack of intact pNIPAM on the surface, possibly from delamination of the films.

The elemental composition determined via XPS indicated the presence of nitrogen on spNIPAM and pNIPAM only

Table 1. Major Elemental Relative Atomic Percentages from XPS Comparing spNIPAM and Control Surfaces^a

	relative atomic percent			
	C	N	O	Si
theoretical	75.0	12.5	12.5	0.0
0.3 wt %	32.4	3.0	45.9	18.6
0.35 wt %	34.9	4.2	41.8	19.0
0.4 wt %	33.2	3.7	43.9	19.2
pNIPAM	76.0	11.2	12.2	0.0
TEOS	35.5	0.0	47.9	16.6
blank Si	8.3	0.0	40.5	51.1

^a $N = 9$ for all surfaces, with a standard deviation of less than 3%.

Table 2. Relative Atomic Percents from High-Resolution C1s Comparing spNIPAM and Control Surfaces^a

	relative atomic percent		
	CH (285 eV)	CO/CN (+1.5)	O=C-N (+3.0)
theoretical	66.7	16.7	16.7
0.3 wt %	61.7	27.5	10.8
0.35 wt %	60.0	27.0	13.0
0.4 wt %	59.7	28.7	11.6
pNIPAM	65.0	22.3	12.7
TEOS	47.0	53.0	0.0
blank Si	95.4	4.6	0.0

^a $N = 9$ for all surfaces with a standard deviation of less than 3%.

surfaces, thus verifying the presence of NIPAM (see Table 1). A similar trend is illustrated in the high-resolution carbon spectrum (see Table 2 and Figure 2) with the C–OH/C–N peaks. Theoretical values determined from the stoichiometry

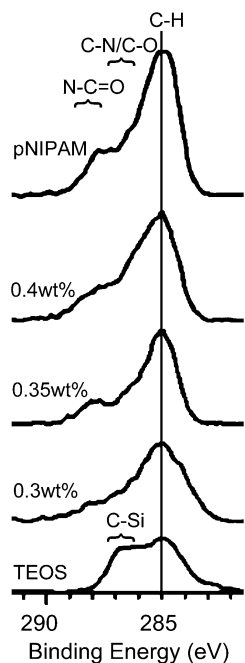


FIGURE 2. Panel of representative high-resolution XPS C1s spectra for pNIPAM only, 0.4 wt % spNIPAM, 0.35 wt % spNIPAM, 0.3 wt % spNIPAM, and TEOS only. The top four spectra all look similar, with peaks at 286.5 and 288 eV indicating successful deposition of pNIPAM.

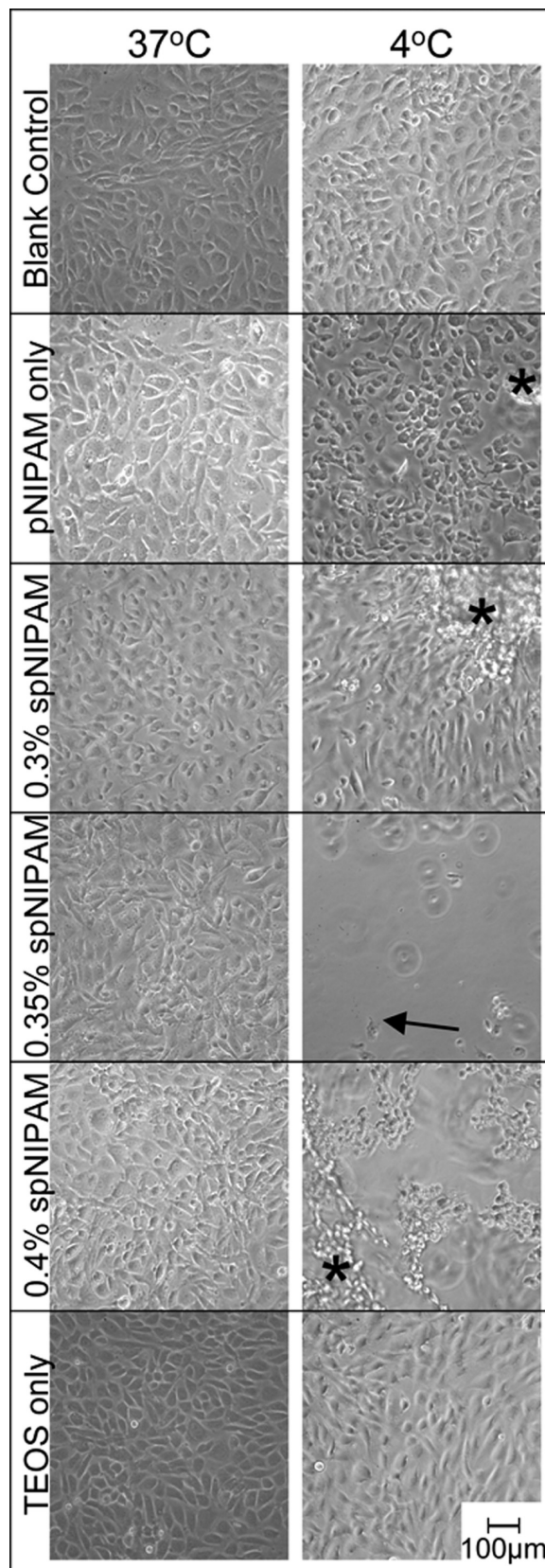


FIGURE 3. Representative cell images after cell detachment procedure showing the most cell detachment from 0.35 wt % spNIPAM. The arrow indicates a cell is still attached to the surface. There was no cell detachment on the blank control slide and moderate detachment from 0.3 wt % spNIPAM and 0.4 wt % spNIPAM surfaces. The asterisks indicate aggregated clumps of cells that are releasing from the surface.

Table 3. Bovine Aortic Endothelial Cell Release from spNIPAM (shaded grey) and Control Surfaces^a

surface	% cell release
0.3 wt %	39.3
0.35 wt %	75.3
0.4 wt %	65.1
pNIPAM	30.4
TEOS	0.0
blank glass	0.0

^a $N = 9$ for all surfaces with a standard deviation less than 2%.

of the monomer (75% C, 12.5% O, 12.5% N) closely match those from the pNIPAM only surfaces (71.8% C, 11.9% O, 9.9% N, 6.4% Si), with the exception of the Si peak. Unlike the spNIPAM surfaces that have Si from TEOS, the Si peak on pNIPAM-only surfaces most likely arises from the underlying Si chip, indicating the film is $<100 \text{ \AA}$ (XPS penetration depth = 100 \AA).

Cellular Response. At $37 \text{ }^\circ\text{C}$, cells adhered and proliferated equally well on all surfaces. After decreasing the temperature to $4 \text{ }^\circ\text{C}$, cells were detached, with the most cell detachment on 0.35 wt % spNIPAM surfaces (see Figure 3 and Table 3). This correlates with the observation that 0.35 wt % spNIPAM also had the only significant contact angle change. In addition, while preparing the sol-gel/pNIPAM for deposition, we observed that in the 0.4 wt % spNIPAM mixtures, the pNIPAM would precipitate out, which would explain a lack of thermoresponsive pNIPAM on those surfaces. In contrast, control surfaces composed of TEOS and blank glass coverslips did not release cells. All surfaces with pNIPAM demonstrated some cell detachment with the least detachment on pNIPAM-only surfaces, suggesting codeposition with TEOS enhances cell release, possibly by stabilizing the films and inhibiting delamination. It is also interesting to note that cells released from the center of surfaces in the form of aggregated clumps, as indicated in Figure 3 by asterisks. This is in contrast to other deposition methods, such as plasma-deposited pNIPAM (ppNIPAM), where the cells release in confluent sheet starting at the edges of the surfaces (25).

CONCLUSIONS

We have successfully adapted a method developed by Rao et al for the deposition of pNIPAM for bioengineering applications. PNIPAM in conjunction with a sol-gel was found to be instrumental in maintaining film integrity during experimentation, where thermoresponse and cell detachment properties were tested. This method allowed for relatively inexpensive and quickly fabricated surfaces. Determination of the amount of pNIPAM to sol-gel demonstrated that 0.35 wt % spNIPAM surfaces had both the best thermoresponse and cell release. Cells detach from the spNIPAM surface as isolated cells or aggregated clumps, which may limit the utility of this technique for cell sheet engineering, where intact sheets are desired; however, this technique is a simple and affordable alternative to previously

described pNIPAM deposition methods for those applications that do not require intact cell sheets, such as protein preconcentration or biofouling release.

Acknowledgment. The authors thank Steven Candelaria, Marta Cooperstein, Dan Graham, Laura Pawlikowski, Venkata Rama Rao, Elsa Romero, and Angela Wandinger-Ness for helpful discussions, contributions, and expertise. This work was supported by NSF-Partnerships for Research and Education in Materials (PREM) program Grant DMR-0611616, Sandia-University Research Program Grant 739577, ONR grants N00014-08-1-0741 and N00014-05-1-0743, as well as funding from 3M Corporation and the UNM Center for Biomedical Engineering. XPS data were obtained by Kateryna Artyushkova. J.A.R. was supported by an NSF Graduate Research Fellowship. S.H. was supported by an NSF REU.

REFERENCES AND NOTES

- Canavan, H. E.; Cheng, X. H.; Graham, D. J.; Ratner, B. D.; Castner, D. G. *J. Biomed. Mater. Res., Part A* **2005**, *75A*, 1–15.
- Reed, J. A.; Lucero, A. E.; Cooperstein, M. A.; Canavan, H. E. *J. Appl. Biomater. Biointerfaces* **2008**, *6*, 81–88.
- Kushida, A.; Yamato, M.; Konno, C.; Kikuchi, A.; Sakurai, Y.; Okano, T. *J. Biomed. Mater. Res.* **2000**, *51*, 216–225.
- Akiyama, Y.; Kikuchi, A.; Yamato, M.; Okano, T. *Langmuir* **2004**, *20*, 5506–5511.
- Canavan, H. E.; Cheng, X. H.; Graham, D. J.; Ratner, B. D.; Castner, D. G. *Plasma Processes Polym.* **2006**, *3*, 516–523.
- Canavan, H. E.; Cheng, X. H.; Graham, D. J.; Ratner, B. D.; Castner, D. G. *Langmuir* **2005**, *21*, 1949–1955.
- Ista, L. K.; Perez-Luna, V. H.; Lopez, G. P. *Appl. Environ. Microbiol.* **1999**, *65*, 1605–1609.
- Cunliffe, D.; Alarcon, C. D.; Peters, V.; Smith, J. R.; Alexander, C. *Langmuir* **2003**, *19*, 2888–2899.
- Okajima, S.; Sakai, Y.; Yamaguchi, T. *Langmuir* **2005**, *21*, 4043–4049.
- Miyagawa, S.; Sawa, Y.; Sakakida, S.; Taketani, S.; Kondoh, H.; Memon, I. A.; Imanishi, Y.; Shimizu, T.; Okano, T.; Matsuda, H. *Transplantation* **2005**, *80*, 1586–1595.
- Chiantore, O.; Guaita, M.; Trossarelli, L. *Makromol. Chem.* **1979**, *180*, 969–973.
- Kubota, K.; Fujishige, S.; Ando, I. *J. Phys. Chem.* **1990**, *94*, 5154–5158.
- Winnik, F. M.; Ringsdorf, H.; Venzmer, J. *Macromolecules* **1990**, *23*, 2415–2416.
- Otake, K.; Inomata, H.; Konno, M.; Saito, S. *Macromolecules* **1990**, *23*, 283–289.
- Priest, J. H.; Murray, S. L.; Nelson, R. J.; Hoffman, A. S. *ACS Symp. Ser.* **1987**, *350*, 255–264.
- Matyjaszewski, K.; Xia, J. H. *Chem. Rev.* **2001**, *101*, 2921–2990.
- Angiolini, L.; Benelli, T.; Giorgini, L.; Paris, F.; Salatelli, E.; Fontana, M. P.; Camorani, P. *Eur. Polym. J.* **2008**, *44*, 3231–3238.
- Hennink, W. E.; van Nostrum, C. F. *Adv. Drug Delivery Rev.* **2002**, *54*, 13–36.
- Takezawa, T.; Yamazaki, M.; Mori, Y.; Yonaha, T.; Yoshizato, K. *J. Cell Sci.* **1992**, *101*, 495–501.
- Kanazawa, H.; Yamamoto, K.; Matsushima, Y.; Takai, N.; Kikuchi, A.; Sakurai, Y.; Okano, T. *Anal. Chem.* **1996**, *68*, 100–105.
- Mizutani, A.; Kikuchi, A.; Yamato, M.; Kanazawa, H.; Okano, T. *Biomaterials* **2008**, *29*, 2073–2081.
- Da Silva, R. M. P.; Mano, J. F.; Reis, R. L. *Trends Biotechnol.* **2007**, *25*, 577–583.
- Rao, G. V. R.; Lopez, G. P. *Adv. Mater.* **2000**, *12*, 1692.
- Rao, G. V. R.; Krug, M. E.; Balamurugan, S.; Xu, H. F.; Xu, Q.; Lopez, G. P. *Chem. Mater.* **2002**, *14*, 5075–5080.
- Cheng, X. H.; Canavan, H. E.; Stein, M. J.; Hull, J. R.; Kweskin, S. J.; Wagner, M. S.; Somorjai, G. A.; Castner, D. G.; Ratner, B. D. *Langmuir* **2005**, *21*, 7833–7841.

AM900821T